



## Impact of external carbon dose on the removal of micropollutants using methanol and ethanol in post-denitrifying Moving Bed Biofilm Reactors

Torresi, Elena; Escolà Casas, Mònica; Polesel, Fabio; Plósz, Benedek G.; Christensson, Magnus; Bester, Kai

*Published in:*  
Water Research

*Link to article, DOI:*  
[10.1016/j.watres.2016.10.068](https://doi.org/10.1016/j.watres.2016.10.068)

*Publication date:*  
2017

*Document Version*  
Peer reviewed version

[Link back to DTU Orbit](#)

### *Citation (APA):*

Torresi, E., Escolà Casas, M., Polesel, F., Plósz, B. G., Christensson, M., & Bester, K. (2017). Impact of external carbon dose on the removal of micropollutants using methanol and ethanol in post-denitrifying Moving Bed Biofilm Reactors. *Water Research*, 108, 95-105. <https://doi.org/10.1016/j.watres.2016.10.068>

---

### General rights

Copyright and moral rights for the publications made accessible in the public portal are retained by the authors and/or other copyright owners and it is a condition of accessing publications that users recognise and abide by the legal requirements associated with these rights.

- Users may download and print one copy of any publication from the public portal for the purpose of private study or research.
- You may not further distribute the material or use it for any profit-making activity or commercial gain
- You may freely distribute the URL identifying the publication in the public portal

If you believe that this document breaches copyright please contact us providing details, and we will remove access to the work immediately and investigate your claim.

**Impact of external carbon dose on the removal of micropollutants using  
methanol and ethanol in post-denitrifying Moving Bed Biofilm Reactors**

Elena Torresi<sup>† 1,2</sup>, Mònica Escolà Casas<sup>† 3</sup>, Fabio Polesel<sup>2</sup>, Benedek G. Plósz<sup>2\*</sup>, Magnus  
Christensson<sup>1\*</sup>, Kai Bester<sup>3\*</sup>

<sup>†</sup> *Joint first authors; \* Corresponding authors: kb@dmu.dk; magnus.christensson@anoxkaldnes.com;*  
*beep@env.dtu.dk;*

<sup>1</sup> Veolia Water Technologies AnoxKaldnes, Klosterängsvägen 11A, SE-226 47 Lund, Sweden

<sup>2</sup> Department of Environmental Engineering, Technical University of Denmark, Bygningstorvet B115, 2800 Kgs. Lyngby, Denmark

<sup>3</sup> Department of Environmental Science, Århus University, Frederiksborgvej 399, 4000 Roskilde, Denmark

**Keywords:** pharmaceuticals; MBBR; carbon source; biofilms; wastewater; denitrification

## 19    **Abstract**

20    Addition of external carbon sources to post-denitrification systems is frequently used in wastewater  
21    treatment plants to enhance nitrate removal. However, little is known about the fate of  
22    micropollutants in post-denitrification systems and the influence of external carbon dosing on their  
23    removal. In this study, we assessed the effects of two different types and availability of commonly  
24    used carbon sources —methanol and ethanol— on the removal of micropollutants. Two laboratory-  
25    scale moving bed biofilm reactors (MBBRs), containing AnoxKaldnes K1 carriers with acclimated  
26    biofilm from full-scale systems, were operated in continuous-flow using wastewater dosed with  
27    methanol and ethanol. Batch experiments with 22 spiked pharmaceuticals were performed to assess  
28    removal kinetics. Acetyl-sulfadiazine, atenolol, citalopram, propranolol and trimethoprim were  
29    easily biotransformed in both MBBRs (biotransformations rate constants  $k_{\text{bio}}$  between 1.2 and 12.9  
30     $\text{L g}_{\text{biomass}}^{-1} \text{d}^{-1}$ ), 13 compounds were moderately biotransformed (rate constants between 0.2 and 2  $\text{L}$   
31     $\text{g}_{\text{biomass}}^{-1} \text{d}^{-1}$ ) and 4 compounds were recalcitrant. The methanol-dosed MBBR showed higher  $k_{\text{bio}}$   
32    (e.g., 1.5 to 2.5-fold) than in the ethanol-dosed MBBR for 9 out of the 22 studied compounds, equal  
33     $k_{\text{bio}}$  for 10 compounds, while 3 compounds (i.e., targeted sulfonamides) were biotransformed faster  
34    in the ethanol-dosed MBBR. While biotransformation of most of the targeted compounds followed  
35    first-order kinetics, removal of venlafaxine, carbamazepine, sulfamethoxazole and sulfamethizole  
36    could be described with a cometabolic model. Analyses of the microbial composition in the  
37    biofilms using 16S rRNA amplicon sequencing revealed that the methanol-dosed MBBR contained  
38    higher microbial richness than the one dosed with ethanol, suggesting that improved  
39    biotransformation of targeted compounds could be associated with higher microbial richness.  
40    During continuous-flow operation, at conditions representative of full-scale denitrification systems  
41    (hydraulic residence time = 2 h), the removal efficiencies of micropollutants were below 35% in  
42    both MBBRs, with the exception of atenolol and trimethoprim (>80%). Overall, this study

43 demonstrated that MBBRs used for post-denitrification could be optimized to enhance the  
44 biotransformation of a number of micropollutants by accounting for optimal carbon sources and  
45 extended residence time.

46

## 47    **1. Introduction**

48    Currently used biological processes in conventional wastewater treatment plants (WWTPs) are  
49    designed to remove organic carbon and nutrients (nitrogen and phosphorus). As organic  
50    micropollutants are gaining attention due to the associated environmental risks (Daughton and  
51    Ternes, 1999; Plósz et al., 2013), the optimization of biological processes for removal of  
52    micropollutants during wastewater treatment is crucial (Joss et al., 2008). Micropollutants (e.g.,  
53    pharmaceuticals and personal care products) are generally recognized as non-growth substrates  
54    (secondary substrates), as they are present in wastewater in too low concentrations ( $\text{ng L}^{-1}$  to  $\mu\text{g L}^{-1}$ )  
55    to support biomass growth (Fischer and Majewsky, 2014; Rittmann, 1992). Therefore, biological  
56    transformation of micropollutants is mainly the result of cometabolic mechanisms, whereby the  
57    removal of non-growth substrates (micropollutants) requires the presence of primary substrates (i.e.,  
58    COD, nutrients) to support biomass growth (Criddle, 1993; Rittmann, 1992). In cometabolism, the  
59    biotransformation of micropollutant is typically catalyzed by non-specific enzymes (e.g., mono- or  
60    di-oxygenases, *N*-acetyltransferases, hydrolases) or by cofactors produced during the microbial  
61    conversion of the primary substrate (Criddle, 1993; Fischer and Majewsky, 2014). Nevertheless, the  
62    interaction between primary substrate and micropollutants is complex and not completely  
63    understood. In fact, the presence of primary substrate has been reported to either enhance the  
64    removal of micropollutants, e.g., by regenerating reductants such as NAD(P)H under aerobic  
65    conditions (Alvarez-Cohen and Speitel, 2001; Liu et al., 2015), or decrease it, due to competitive  
66    enzyme inhibition (Fischer and Majewsky, 2014; Plósz et al., 2010).

67

68    Recent studies have proposed biofilm systems, e.g., moving bed biofilm reactors (MBBR), as a  
69    promising alternative to activated sludge systems (CAS) with respect to the attenuation of  
70    micropollutants (Escolà Casas et al., 2015a; Falås et al., 2012; Hapeshi et al., 2013; Torresi et al.,

2016). In general, most of the studies concerning the removal of micropollutants during biological wastewater treatment have focused on aerobic systems, whereas only little information is available for anoxic denitrifying conditions: Plósz et al., 2010; Su et al., 2015; Falås et al. 2013, Suárez et al., 2010. While pharmaceuticals such as diclofenac, metoprolol, erythromycin and roxithromycin were found to be transformed mainly under aerobic conditions in activated sludge using synthetic wastewater (Suárez et al., 2010) and in hybrid biofilm-activated sludge processes (Falås et al., 2013), some of the investigated chemicals had similar (i.e., bezafibrate, atenolol, clarithromycin and N<sup>4</sup>-acetylsulfamethoxazole) or higher (i.e., levetiracetam) biotransformation under anoxic conditions than under aerobic ones (Falås et al., 2013). Hence, anoxic biological processes in conventional WWTPs should be considered as a potential step to optimize removal of micropollutants.

The type of carbon source is known to have a strong impact on the structure of denitrifying microbial communities and thus on denitrification efficiency (Baytshtok et al., 2009; Hagman et al., 2007; Lu et al., 2014). This has specific relevance to post-denitrification reactors in full-scale WWTPs, where nitrate removal is achieved by dosing external carbon sources such as methanol and ethanol (Louzeiro et al, 2002; Santos et al., 2001). Methanol and ethanol are metabolized by denitrifying bacteria through different pathways. Methanol undergoes the metabolic reaction of single-carbon compounds, which is exclusive to methylotrophs because of their unique key enzyme (methanol dehydrogenase) that catalyzes the oxidization of methanol to formaldehyde (Anthony et al., 1982, 2011). Instead, ethanol is easily converted by bacterial cells to Acetyl-CoA before entering the glyoxylate cycle (Anthony et al., 2011). Thus, microbial communities in post-denitrifying systems using either of these carbon sources may be fundamentally different and potentially exhibit a different biodiversity and functionality with more or less microbial specialists able to biotransform organic micropollutants. Additionally, biodiversity in terms of species richness

95 (the number of species) and evenness (the relative abundance of the species) (Wittebolle et al.,  
96 2009) was shown to positively associate with the biotransformation of a number of micropollutants  
97 in aerobic activated sludge (Johnson et al., 2015; Stadler and Love, 2016) and nitrifying MBBRs  
98 (Torresi et al., 2016). Further investigation of the impact of biodiversity in different biological  
99 treatment systems seems thus required.

100 In this study, we evaluated the elimination of selected micropollutants (i.e., pharmaceuticals) in  
101 laboratory-scale post-denitrifying MBBRs dosed with methanol or ethanol. Biotransformation  
102 kinetics and removal efficiencies were assessed through targeted batch experiments and during  
103 continuous-flow MBBR operation, respectively. The objectives of our study were: (i) to investigate  
104 the impact of different types of external carbon sources (methanol and ethanol) for post-  
105 denitrification on micropollutant biotransformation; (ii) to assess the structure of the denitrifying  
106 microbial community of MBBR biofilms, following continuous dosing with either methanol or  
107 ethanol; and (iii) to evaluate the influence of organic substrate availability on the transformation of  
108 micropollutants and the related mechanisms, i.e. competitive inhibition and cometabolic  
109 enhancement.

110

## 111 **2. Materials and Methods**

112

### 113 **2.1 Description of the post-denitrifying systems**

114 Two Swedish WWTPs, i.e., Sjölanda and Klagshamn are currently dosing methanol or ethanol,  
115 respectively, as external carbon source in two-stage post-denitrification MBBRs. Thus, two  
116 laboratory-MBBRs were built to resemble such post-denitrification stages, using carriers  
117 (AnoxKaldnes K1) from the first post-denitrification tank of the respective WWTPs already adapted  
118 to methanol and ethanol dosing. The WWTPs are described in Section S1 of the SI (Supporting

Information). Both laboratory-MBBRs (1 L) were operated in continuous feeding of the same wastewater, which was collected after the (aerobic) nitrification step (trickling filter) of Sjölanda WWTP (Lund, Sweden). Thus, during continuous-flow operation, only the indigenous nitrate and nitrite present in the wastewater (averaged concentration of 13 and 1.2 mg L<sup>-1</sup> respectively) were used for denitrification. The filling rate of both reactors was 40%, giving a surface of 0.2 m<sup>2</sup>. The amount of indigenous micropollutants in the reactor influents (consisting in the collected wastewater and feed containing carbon-source) was analyzed. Twelve compounds were quantified giving concentrations between 0.04 µg L<sup>-1</sup> (trimethoprim) and 78 µg L<sup>-1</sup> (iohexol). Complete details of these results are given in Table S6 (SI).

The reactors were continuously flushed with nitrogen gas and stirred for the mixing of the carriers and to strip eventual residual dissolved oxygen. Both reactors were kept at 15°C using a water bath. The feed wastewater was mixed and kept at 4°C during the whole experiment. Phosphate was added to the feed to reach a concentration of 0.5 mg L<sup>-1</sup> to ensure biofilm growth on the carriers. Micropollutant removal and denitrification rates in MBBRs were assessed in two main experiments: (i) batch conditions (24 h) and (ii) continuous-flow operation (2 months). The carbon availability of ethanol and methanol into the two MBBRs was defined as the ratio between the influent loading of organic carbon (COD<sub>added</sub>) and the native loading of nitrate (NO<sub>3</sub>-N<sub>influent</sub>) in the wastewater samples. Optimum COD<sub>added</sub>/NO<sub>3</sub>-N<sub>influent</sub> ratio (gCOD gN<sup>-1</sup>) for complete denitrification is typically around 4 (Metcalf & Eddy, 2003).

## 2.2 Analytical methods

All the samples taken for analysis of conventional pollutants (NH<sub>4</sub><sup>+</sup>-N, NO<sub>3</sub><sup>-</sup>-N, NO<sub>2</sub><sup>-</sup>-N, soluble COD and PO<sub>3</sub><sup>4-</sup>) in batch and continuous experiments were filtered through 0.45 µm glass fiber



143 filters (Sartorius, Göttingen, Germany). Total COD and total nitrogen were analyzed on the  
144 unfiltered sample. All samples were prepared in Hach Lange kits (LCK 303, LCK 339, LCK 341  
145 and LCK 342) and analyzed in a Hach Lange DR2800 spectrophotometer. DO, pH and temperature  
146 in the reactors were measured at each sampling occasion, using a Hach HQ40d multi DO probe and  
147 a HANNA H1991001 pH-meter. The attached biomass concentrations were calculated from the  
148 difference in weight of 3 dried carriers (105 °C for >24 h) before and after biofilm removal (in 2M  
149 H<sub>2</sub>SO<sub>4</sub>) with subsequent brushing (see Figure S2 for results), as previously considered (Escolà  
150 Casas et al., 2015a; Falås et al., 2012; Torresi et al., 2016). Samples for micropollutants were frozen  
151 at -20 °C prior analysis and analyzed via direct injection using HPLC-MS/MS as described in  
152 Escolà Casas et al. (2015a). Information regarding sample preparation, HPLC, mass spectrometry  
153 data, LOD and LOQ of compounds are shown in Escolà Casas et al. (2015a) and in Section S2 (SI).

154

## 155 **2.3 Chemicals**

156 Twenty-two relevant micropollutants (i.e., pharmaceuticals) were selected for this study.  
157 Information regarding CAS numbers and chemical suppliers is found in the supplementary  
158 information in Escolà Casas et al. (2015b). The pharmaceuticals included: (i) four beta-blockers,  
159 i.e., atenolol, metoprolol, propranolol and sotalol; (ii) five X-ray contrast media, i.e., diatrizoic acid,  
160 iohexol, iopamidol, iopromide, iomeprol; (iii) three sulfonamides, i.e., sulfadiazine, sulfamethizole  
161 and sulfamethoxazole and the metabolite acetyl-sulfadiazine; (iv) three analgesics, i.e., phenazone,  
162 diclofenac and ibuprofen; (v) three anti-epileptics/anti-depressants, i.e., carbamazepine, venlafaxine  
163 and citalopram; (vi) four antibiotics, i.e., erythromycin, clarithromycin, trimethoprim and  
164 roxithromycin.

165

166

## 167    **2.4 Batch experiment**

168    To investigate how the type of dosed carbon source influences the removal of micropollutants in  
169    post-denitrifying MBBR, batch experiments were performed in the same reactors used during  
170    continuous-flow operation. These experiments were conducted after 3.5 months of continuous-flow  
171    operation of the two systems. During the batch experiments, a  $\text{COD}_{\text{added}}/\text{NO}_3\text{-N}_{\text{influent}}$  ratio of 3.4 for  
172    both reactors was adopted to obtain excess concentration of nitrate. Anoxic conditions were  
173    maintained by flushing the reactors with nitrogen gas during the experiment. The feed used for the  
174    batch consisted of the same wastewater used in continuous operation spiked with  $239 \pm 2$  mg  
175     $\text{COD L}^{-1}$  of methanol for the methanol-dosed reactor and the same amount of ethanol for the  
176    ethanol-dosed reactor,  $70 \pm 3$  mg  $\text{NO}_3\text{-N L}^{-1}$  in form of sodium nitrate and 22 micropollutants with  
177    an initial nominal concentration of  $2 \mu\text{g L}^{-1}$ . The micropollutants were added from a stock solution  
178    ( $40 \text{ mg L}^{-1}$  in methanol). To minimize the increase of COD concentration in the batch feed due to  
179    the methanol from the stock solution, the micropollutant solution was first spiked into an empty  
180    glass beaker and the methanol was let to evaporate for approximately 1 hour. Afterwards, the feed  
181    was added to the beaker containing the micropollutants and mixed to re-dissolve the  
182    micropollutants. The batch experiment lasted 24 hours and samples for conventional and  
183    micropollutants analysis were taken at regular intervals. To keep the biomass concentration constant  
184    during the experiment, three carriers were withdrawn from the reactors each time a sample was  
185    taken for analysis. The pH value in both reactors was continuously measured and adjusted to 7.5  
186    using 1M HCl. The temperature was kept constant at  $15^\circ\text{C}$ .

187

### 188    ***2.4.1 Denitrification during batch experiment***

189    Denitrification rates normalized on surface area of reactors  $r_{\text{NO}_3,2\text{-N}}$  ( $\text{gNO}_{3,2\text{-N m}^{-2} \text{ d}^{-1}}$ ) and specific  
190    denitrification rates accounting for the biomass  $k_{\text{NO}_3,2\text{-N}}$  ( $\text{gNO}_{3,2\text{-N g}_{\text{biomass}}^{-1} \text{ d}^{-1}$ ) were derived

191 through linear regression using  $\text{NO}_3^-$ -N and  $\text{NO}_2^-$ -N measurements during batch experiment. An  
192 accumulation of nitrite in the systems was noticed ( $\sim 6 \text{ mg L}^{-1}$ ), therefore  $\text{NO}_{3,2}$ -N utilization curves  
193 accounting also for  $\text{NO}_2^-$ -N concentration were derived accordingly to Sözen et al. (1998).

194  
195 A two step-denitrification activated sludge model (ASM) was used to describe up-take of primary  
196 substrates (i.e., readily soluble biodegradable COD ( $S_S$ ), soluble nitrate ( $S_{\text{NO}_3}$ ) and nitrite ( $S_{\text{NO}_2}$ ))  
197 which was extended with the Activated Sludge Model for Xenobiotics ASM-X (Plósz et al., 2012;  
198 Polesel et al., 2016) to determine micropollutant biotransformation rates (Table 1). Readily soluble  
199 biodegradable COD ( $S_S$ ) was determined as the difference between soluble COD (sCOD)—  
200 measured during the experiments—and soluble inert COD ( $S_I$ )—calculated according to Roozeveld  
201 and Van Loosdrecht (2002). The ASM for denitrification was adapted from Pan et al. (2015) and  
202 included two process rate equations with reduction of nitrate to nitrite (R1) and nitrite to nitrogen  
203 (R2) (Table 1). Parameters that could not be identified through model calibration to experimental  
204 results (maximum specific growth rates  $\mu_H$ , affinity constants for substrate— $K_{S1}$  and  $K_{S2}$ —and for  
205 nitrogen species— $K_{\text{NO}_3}^{\text{HB}}$  and  $K_{\text{NO}_2}^{\text{HB}}$  —) were adopted from literature (Hiatt and Grady, 2008).  
206 Parameters that are known to be sensitive to the experimental data (i.e., heterotrophic yields  $Y_H$ ,  
207 anoxic growth factors for the process 1 and 2,  $\eta_{g1}$  and  $\eta_{g2}$ ) were calibrated. Definition of the  
208 components and model calibration are presented in Section S3 and Table S1 (SI). The model was  
209 implemented in AQUASIM 2.1d (Reichert et al., 1994) and the parameters were estimated using the  
210 secant method embedded.

211

#### 212 ***2.4.2 Micropollutants removal kinetics during batch experiment***

213 Model structures to assess biotransformation rate of micropollutants were identified using the ASM-  
214 X as modelling framework (Polesel et al., 2016; Plósz et al., 2010, 2012, 2013). The framework

215 used in this study is summarized in Table 1 and included processes such as parent compound  
 216 retransformation (e.g., deconjugation of human metabolites) (1), biotransformation (2) and  
 217 cometabolic biotransformation (in the presence and absence of organic growth substrate) (3). The  
 218 effect of diffusion into biofilm on the removal of pharmaceuticals from bulk aqueous phase was  
 219 lumped in the biotransformation rate constants, as previously considered by Falås et al. (2012,  
 220 2013), Escolá Casas et al. (2015a) and Hapeshi et al. (2013). The cometabolic process was  
 221 modelled as proposed by Plósz et al. (2012), using pseudo-first order kinetics with respect to  
 222 micropollutant concentration and estimating two biokinetics: (i) the cometabolic biotransformation  
 223 rate constant  $q_{\text{bio}}$  in the presence of the primary substrate and (ii) biotransformation rate constant  
 224  $k_{\text{bio}}$  in the absence of primary substrate. Accordingly, biotransformation kinetics of the cometabolic  
 225 substrate (e.g., micropollutant) depend on the primary substrate concentration (e.g., organic matter  
 226 expressed as readily soluble biodegradable COD,  $S_S$ ) considered a co-limiting substrate. In Table 1  
 227  $C_{\text{LI}}$  and  $C_{\text{CJ}}$  denote the aqueous concentration ( $\text{ng L}^{-1}$ ) of the parent compound and the human  
 228 metabolites undergoing deconjugation to the parent compound, respectively. The retransformation  
 229 rate constant  $k_{\text{Dec}}$  ( $\text{L g}_{\text{biomass}}^{-1} \text{d}^{-1}$ ) defines kinetics of retransformation to parent compound. Sorption  
 230 processes were also included considering the sorption coefficient  $K_D$  ( $\text{L g}_{\text{biomass}}^{-1}$ ) which was  
 231 calibrated using values from previous studies estimated under denitrifying condition when available  
 232 (Table S2 in SI). As to the best of our knowledge values of  $K_D$  were not previously estimated for  
 233 biofilm under denitrifying conditions,  $K_D$  measured for activated sludge were used in this study.  
 234 The half-saturation coefficient for  $S_S$ , ( $K_S$ ) in Table 1, was retrieved from Hiatt and Grady (2008).  
 235  $X_{\text{biomass}}$  ( $\text{g}_{\text{biomass}} \text{L}^{-1}$ ) denoted the biomass concentration in the MBBRs and growth of biomass on  
 236 micropollutants was considered negligible.

237

238 Biotransformation constants  $k_{\text{bio}}$  (process 2, Table 1) were estimated from the measured data using  
239 least-square optimization without weighting in GraphPad Prism 5.0. Parent compound  
240 retransformation and cometabolism model (processes 1 and 3, Table 1) were implemented in  
241 AQUASIM 2.1d (Reichert et al., 1994) and the parameters were estimated using the secant method  
242 embedded.

243 Removal rate constants  $k$  ( $\text{d}^{-1}$ ) were also estimated to compare the performance of the two MBBR  
244 systems, regardless of biomass concentration and sorption processes (Escolà Casas et al., 2015a,b).  
245 For the chemicals following cometabolism model (and thus exhibiting two biokinetics),  $k$  was  
246 calculated considering the estimated  $q_{\text{bio}}$ . Differences between biotransformation rate constants of  
247 the two MBBRs were assessed by examining the overlap between standard deviations of the  
248 estimated values (Cumming et al., 2007).

249

## 250 **2.5 DNA extraction, PCR amplification, sequencing and bioinformatics analysis.**

251 One carrier was collected from each MBBR before the batch experiment and stored in a sterilized  
252 Eppendorf tube at  $-20^{\circ}\text{C}$ . Biomass was detached using a sterile brush (Gynobrush, Dutscher  
253 Scientific, United Kingdom) using tap water and consequently centrifuged (10000 rpm for 5  
254 minutes) to remove excess water. DNA extraction, PCR amplification (using 16S rRNA bacteria  
255 gene primers) and Illumina sequencing were performed as described in Section S5 of the SI.  
256 Taxonomic assignment and calculation of alpha diversity metrics (Shannon biodiversity and ACE  
257 extrapolated richness) were performed in mothur using the RDP reference taxonomy. Additional  
258 diversity indices were calculated according to Hill et al. (1973). Microbial evenness was estimated  
259 as  $H_1/H_0$  as described in Johnson et al. (2015).

260

## 261 2.6 Continuous-flow experiment

262 The two MBBRs used for the present study were operated for over 4 months. The MBBRs were  
263 kept with a  $COD_{added}/NO_3-N_{influent}$  ratio equal to 3 (close to the ratios used at the respective  
264 WWTPs) for the first two weeks of operation. The fraction of inert COD was taken into account (by  
265 subtracting it from the amount of available biodegradable COD) when planning experiments under  
266 carbon limitation. A hydraulic retention time (HRT) of 2 hours was set similar to the HRT used at  
267 the full-scale WWTPs. After two weeks of acclimatization, baseline carbon-dosage periods of  
268  $COD_{added}/NO_3-N_{influent}$  were alternated with short carbon-dosage periods (~5 days) to avoid biomass  
269 adaptation. Accordingly, concentrations of methanol and ethanol in the feed solutions were changed  
270 to test  $COD_{added}/NO_3-N_{influent}$  ratios ranging from 1 to 5, while keeping constant HRT. This test  
271 phase lasted about 2 months. The  $COD_{added}/NO_3-N_{influent}$  ratios and the dates are reported in the  
272 Table S3 (SI). The range of  $COD_{added}/NO_3-N_{influent}$  ratios was chosen to assess carbon limiting  
273 condition at low  $COD_{added}/NO_3-N_{influent}$  ratio and not far exceeding the stoichiometric  
274  $COD_{added}/NO_3-N_{influent}$  ratio needed for complete denitrification. The denitrification rate  $r_D$  ( $gN\ d^{-1}$   
275  $m^{-2}$ ) in continuous operation, was calculated for each carbon-dosage test by using the Equation S1  
276 (Section S6, SI). Micropollutant removal efficiency (“measured removal” in Figure 4) was  
277 calculated as difference between inlet and outlet concentrations. Micropollutant removal efficiency  
278 during continuous operation (“predicted removal” in Figure 4) was predicted using removal rate  
279 constant  $k$  ( $d^{-1}$ ) estimated during batch experiment according to Equation 1:

$$280 \quad Removal\ (\%) = \left( 1 - \left( \frac{1}{(1+k_i \cdot HRT)} \right) \right) \cdot 100 \quad \text{Equation 1}$$

281

## 282    **3. Results and discussion**

283

### 284    **3.1 Batch experiment**

285

#### 286    ***3.1.1 Denitrification kinetics***

287    Denitrification rates ( $r_{\text{NO}_3,2\text{-N}}$ ,  $k_{\text{NO}_3,2\text{-N}}$ ) were derived through linear regression of measured  $\text{NO}_3^-$ -N  
288    and  $\text{NO}_2^-$ -N concentration during batch experiment (Figure S5, SI). The ethanol-dosed reactor  
289    presented a higher surface-normalized denitrification rate  $r_{\text{NO}_3,2\text{-N}}$  (Table 2) than the methanol driven  
290    one, which is in agreement with previous studies (Santos et al., 2001; Christensson et al., 1994).  
291    This is likely due to the higher growth yield expected using ethanol thereby leading to higher  
292    biomass production per surface area in ethanol-dosed systems (Mokhayeri et al., 2009). On the  
293    other hand, denitrification rates ( $k_{\text{NO}_3,2\text{-N}}$ ) normalized by biomass weight (higher for the ethanol-  
294    dosed reactor) were comparable in the two MBBRs, suggesting similar activity in terms of nitrate  
295    and nitrite removal in the two biofilms.

296

#### 297    ***3.1.2 Micropollutant removal kinetics***

298    Biotransformation kinetics of most of the investigated chemicals could be described with first-order  
299    equation (Table 1, process 2), thereby allowing for the estimation of removal rates  $k$  ( $\text{d}^{-1}$ ) and  
300    pseudo-first order biotransformation rate constants  $k_{\text{bio}}$  ( $\text{L g}_{\text{biomass}}^{-1} \text{d}^{-1}$ ). Abiotic transformation  
301    processes were previously investigated by the authors using plastic (polyethylene) carriers  
302    (AnoxKaldnes Z-carriers) and effluent wastewater (Torresi et al., 2016), suggesting no significant  
303    impact of abiotic processes (e.g., abiotic hydrolysis, volatilization, sorption onto plastic or glass) on  
304    the removal of several targeted micropollutants (Figure S9). Figures 1 and S1 summarize measured  
305    and simulated micropollutant concentration profiles during batch experiments.

306 The removals of erythromycin, clarithromycin, venlafaxine, carbamazepine, sulfamethoxazole and  
 307 sulfamethizole was predicted using (i) a pseudo-first order biotransformation model (Table 1,  
 308 process 2), with no interaction (inhibition/enhancement) between micropollutant and primary  
 309 substrate; and (ii) additionally, a cometabolic model (Table 1, process 3), assuming that the  
 310 turnover of the micropollutants is enhanced by the presence of primary substrate. Predictions with  
 311 the two models are presented in Figure 1b–d using dashed lines and solid lines, respectively. The  
 312 goodness of the two model fits ( $R^2$ ) is summarized in Table S4 (SI). For erythromycin and  
 313 clarithromycin, the cometabolic model ( $R^2 > 0.9$ ) provided only for a marginal improvement of the  
 314 fitting compared to the pseudo-first order biotransformation model ( $R^2 > 0.8$ ), making it difficult to  
 315 draw conclusion on the removal mechanism of these two compounds. However, the prediction of  
 316 carbamazepine's removal was significantly improved by adopting the cometabolic model ( $R^2 > 0.9$ )  
 317 compared to the pseudo first-order biotransformation model ( $R^2 < 0.5$ ) in both MBBRs.  
 318 Cometabolic biotransformation of carbamazepine has been previously observed in aerobic and  
 319 anoxic activated sludge (Plósz et al., 2012) with cometabolic biotransformation rate constant  $q_{\text{bio}}$   
 320 ( $1.2 \text{ L g}^{-1} \text{ d}^{-1}$  under anoxic condition), in close agreement with our results. Similarly, the removal of  
 321 venlafaxine, sulfamethoxazole and sulfamethizole removal was better predicted using the  
 322 cometabolic model ( $R^2 > 0.9$ ). In Figure 1a, the measured and simulated concentration of soluble  
 323 COD (sCOD), nitrate ( $\text{NO}_3\text{-N}$ ) and nitrite ( $\text{NO}_2\text{-N}$ ) and simulated readily biodegradable COD ( $S_s$ )  
 324 are reported. For the abovementioned micropollutants,  $S_s$  limitation (approximately after 3 hours  
 325 from the beginning of the experiment) corresponded to a change in biotransformation kinetics.  
 326 Interestingly, in the ethanol-fed reactor, the modelled  $S_s$  limitation coincided with a significant  
 327 decrease in the biotransformation rates of sulfamethoxazole and sulfamethizole (Figure 1d right),  
 328 thereby leading to a rather low removal rate during the rest of the experiment. A similar effect for  
 329 both compounds, though at lower extent, was observed for the methanol-dosed reactor.



330 Cometabolic transformation of trace chemicals was previously shown in suspended cultures under  
331 aerobic, anaerobic and anoxic conditions (Delgadillo-Mirquez et al., 2011; Fernandez-Fontaina et  
332 al., 2014; Plósz et al., 2010; Popat and Deshusses, 2011; Tran et al., 2013). Removal via  
333 cometabolism was previously observed for sulfamethoxazole in nitrifying (Kassotaki et al., 2016;  
334 Müller et al., 2013) and in aerobic and anoxic activated sludge (Alvarino et al., 2016), as well as for  
335 erythromycin and roxithromycin (Fernandez-Fontaina et al., 2014) in nitrifying activated sludge.  
336 Thus, our results support the hypothesis that the change of primary substrate availability can  
337 significantly impact the removal of a number of micropollutants as a result of cometabolic  
338 mechanisms under denitrifying conditions.

339

340 While the other sulfonamides followed cometabolic biotransformation, the removal of sulfadiazine  
341 was different. It could not be described with first-order kinetics ( $R^2 < 0.2$  and  $< 0.4$  for methanol-  
342 and ethanol-dosed MBBR respectively, dashed lines in Figure 1 e), due to the presence of its  
343 conjugate acetyl-sulfadiazine. Acetyl-sulfadiazine is the main human metabolite of sulfadiazine  
344 (Vree et al., 1995) and it has been previously observed to undergo de-acetylation (Zarfl et al.,  
345 2009), similarly to other acetyl-sulfonamides such as  $N^4$ -acetylsulfamethoxazole (Göbel et al.,  
346 2007). For these chemicals, a model including retransformation (deconjugation) of acetyl-  
347 sulfadiazine to sulfadiazine and concurrent biotransformation of sulfadiazine was used to estimate  
348 biotransformation rate constants  $k_{bio}$  for sulfadiazine and retransformation rate constant  $k_{Dec}$  for  
349 acetyl-sulfadiazine (Table 1, processes 1 and 2). However, this modelling approach did not  
350 adequately describe the concentration changes of sulfadiazine in any of the MBBRs ( $R^2 < 0.2$ ,  
351 continuous lines in Figure 1e):

352 For the methanol-dosed MBBR, acetyl- sulfadiazine was decreasing rapidly and sulfadiazine (being  
353 formed from acetyl-sulfadiazine) reached a maximum before being slowly further biotransformed

(Figure 1e left). In the ethanol-dosed MBBR, the acetyl-sulfadiazine was also rapidly removed and sulfadiazine concentration did never increase. Thus, for the ethanol-dosed reactor there is no indication for a deconjugation reaction of acetyl-sulfadiazine to sulfadiazine, while that is partially possible in the methanol-dosed one. Hence, the transformation of acetyl-sulfadiazine probably occurred partially following another metabolic pathway leading to the formation of other (undetected) transformation products. To test whether other pathways could be possible, the EAWAG-BBD pathway prediction systems (EAWAG-BBD, 2016) was used: It showed the possible transformation of acetyl-sulfadiazine to other transformation products, e.g., 2-aminopyrimidine and 4-aminobenzenesulfonic acid (Figure S6, SI). However, additional research on the different transformation pathways of acetyl-sulfadiazine in the two tested MBBRs is needed to substantiate this hypothesis. Further discussion on the biotransformation of acetyl-sulfadiazine and sulfadiazine in the two investigated MBBRs is reported in S4 in SI.

366

367

### 3.2. Influence of dosed carbon-source on microbial communities

We analyzed the biofilm microbial community of the two different MBBRs by 16S rRNA amplicon sequencing. After implementation of quality control measures, a total of 10847 high quality sequences were obtained with an average length of 460 bp. Subsequently, the number of reads of each sample was normalized to 4562 sequences and clustered into an average of 690 observed OTUs at 97% sequence similarity per sample (cut-off level of 3%). The facultative methanol-utilizing  $\beta$ -Proteobacteria, *Methylophilus*, was identified as the main relative abundance genus (24%) in the methanol-dosed reactor (Figure 2)—a result that closely agreed with previous studies on methanol-dosing denitrification systems (Baytshtok et al., 2009; Jenkins et al., 1987; Lu et al., 2014). For the biofilm grown in the ethanol-dosed reactor, *Arcobacter* and *Thiothrix* genus exhibited 23% and 9% relative abundance, respectively. *Arcobacter* was previously identified in

379 full-scale MBBRs treating municipal wastewater (Biswas and Turner, 2012). *Thiothrix* is known to  
 380 degrade sulfur containing compounds and it was suggested to influence the removal of sulfa-based  
 381 antibiotics in membrane bioreactors (Xia et al., 2012). Microbial community diversity in the two  
 382 MBBRs was evaluated by comparing Shannon diversity and evenness indices. We observed no  
 383 major difference in the methanol- and ethanol-dosed reactors between Shannon diversity indices  
 384 ( $4.153 \pm 0.05$  and  $4.184 \pm 0.03$ , mean and standard deviation, respectively) and evenness ( $0.092 \pm$   
 385  $0.002$  and  $0.095 \pm 0.001$ , respectively) (Figure 2, Table S5 of the SI). Similar values of Shannon  
 386 diversity indices were found previously in aerobic nitrifying MBBRs (Bassin et al., 2015; Torresi et  
 387 al., 2016). On the other hand, the extrapolated taxonomic richness ACE in the methanol- and  
 388 ethanol-dosed reactors were estimated to be  $999 \pm 103$  and  $781 \pm 87$  OTUs, respectively, thus  
 389 suggesting slightly differences between the microbial richness of the two biofilms (Figure 2).  
 390 Similar evidence was obtained from nitrite reductase *nirK*- and *nirS*-based restriction fragment  
 391 length polymorphism (RFLP) analysis on activated sludge supplemented with methanol or ethanol,  
 392 with higher diversity in terms of richness of *nirS* genotypes observed in the methanol-dosed sludge  
 393 (Hallin et al., 2006).

394

### 395 **3.3. Influence of dosed carbon source on micropollutants biotransformation**

396 A comparative assessment of the estimated  $k_{\text{bio}}$ ,  $q_{\text{bio}}$  and  $k_{\text{Dec}}$  values for the methanol- and ethanol-  
 397 dosed MBBRs is shown in Figure 3. For 9 compounds the estimated values of biotransformation  
 398 and cometabolic transformation rate constants ( $k_{\text{bio}}$  and  $q_{\text{bio}}$ ) for the methanol-dosed MBBR were  
 399 higher (1.5 to 2.5-fold) than those from the ethanol-dosed reactor (namely atenolol, citalopram,  
 400 trimethoprim, ibuprofen, iopromide, metoprolol, iohexol, iomeprol, sotalol, venlafaxine).  
 401 Conversely, the sulfonamides acetyl-sulfadiazine, sulfamethoxazole, sulfamethizole were  
 402 transformed at higher rate constants (up to 2.8-fold) in the ethanol-dosed reactor. The remaining 10

403 compounds behaved similarly in both reactors. We further classified the biotransformation potential  
404 of the targeted micropollutants of the two denitrifying MBBRs in three groups (Table 3): easily  
405 degradable ( $q_{\text{bio}}$  and  $k_{\text{bio}} > 2$ ), moderately degradable ( $0.2 \leq k_{\text{bio}}$  and  $q_{\text{bio}} \geq 2$ ) and hardly degradable  
406 ( $k_{\text{bio}}$  and  $q_{\text{bio}} < 0.2$ ).

407 We observed that some of the targeted chemicals classified as easily degradable (propranolol,  
408 atenolol, citalopram) presented removal rate constant  $k$  ( $\text{d}^{-1}$ ) above  $10 \text{ d}^{-1}$  and similar between the  
409 two MBBRs (Table 3). As the two MBBRs presented different amount of biomass (Table 2) during  
410 batch experiment, the lower values of  $k_{\text{bio}}$  for the high degradable compounds in the ethanol-dosed  
411 reactor could mainly derive from the normalization to a higher amount of biomass prevailing in the  
412 ethanol-dosed reactor.

413 On the other hand, a number of moderately degradable chemicals (i.e., X-ray contrast media,  
414 ibuprofen, metoprolol and sotalol) were associated to  $k$  and  $k_{\text{bio}}$  values approximately two times  
415 higher in the methanol-dosed than in the ethanol-dosed reactor. The two biofilm microbial  
416 communities likely played an important role on the biotransformation of these chemicals. As  
417 previously described (Section 3.2), the higher microbial richness observed in the biofilm enriched  
418 with methanol could have likely contributed to the overall higher micropollutant biotransformation  
419 in the methanol-dosed MBBR. Similarly, positive associations between biodiversity and the rates of  
420 specific micropollutant biotransformations were observed in activated sludge (Johnson et al., 2015;  
421 Stadler and Love, 2016) and MBBR (Torresi et al., 2016).

422 No major differences were observed between the biotransformation rate constants  $k_{\text{bio}}$  of the hardly  
423 degradable compounds (diatrizoic acid, iopamidol, diclofenac and phenazone) in the two MBBRs,  
424 suggesting that their removal is neither biomass nor carbon source dependent.

425

### 3.4 Highlighted compounds

Among the X-ray contrast media, iopamidol and diatrizoic acid were found to be recalcitrant in both reactors during batch experiment (Figure S1, SI), while iomeprol, iohexol and iopromide were found moderately degradable (Figure 1d). These results are in agreement with previous studies conducted with aerobic MBBRs (Escolà Casas et al., 2015a; Hapeshi et al., 2013). Our results show that denitrifying MBBRs could effectively remove iomeprol, iohexol and iopamidol, with  $k_{\text{bio}}$  comparable to studies on activated sludge (Joss et al., 2006; Onesios et al., 2009)

The analgesic ibuprofen exhibited lower biotransformation rate constants (Table 3) than the ones obtained in previous studies under aerobic conditions (Escolà Casas et al., 2015a,b; Falås et al., 2012; Torresi et al., 2016) as ibuprofen is easily degraded under aerobic conditions. Other analgesics, i.e., phenazone and diclofenac, have also previously observed to be hardly degradable in both aerobic MBBR and activated sludge (Escolà Casas et al., 2015a; Joss et al., 2006). Nevertheless,  $k_{\text{bio}}$  values for diclofenac were reported to be higher under nitrifying conditions in both biofilms and activate sludge (Torresi et al., 2016; Tran et al., 2009) than as obtained in this study under denitrifying conditions, thus indicating limited diclofenac removal under anoxic conditions.

In the batch experiment, citalopram was fully removed in both reactors within 0.4 days (Figure 1b), resulting in a  $k_{\text{bio}}$  of  $2.3 \text{ L d}^{-1} \text{ g}_{\text{biomass}}^{-1}$  (Table 3). Similar biotransformation kinetics was found in aerobic MBBR (Escolà Casas et al., 2015a) and sludge (Suárez et al., 2012), while anoxic CAS showed lower kientics compared to the one obtained in th anoxic MBBRs of this study. At HRTs higher than 0.4 days, a removal efficiency of 65% was achieved in a complete autotrophic nitrogen removal process (Alvarino et al., 2015). In our study, predicted removal efficiency of citalopram (at HRT of 0.4 days) was calculated to be >80% in both reactors (Equation 1) during continuous-flow

operation. Furthermore, in denitrifying activated sludge reactors a  $k_{\text{bio}}$  of  $0.5 \text{ L d}^{-1} \text{ g}_{\text{biomass}}^{-1}$  was obtained for citalopram (Suárez et al., 2010) and a removal of 44 % under anoxic condition (Suárez et al., 2010).

The removal of carbamazepine and venlafaxine (with  $q_{\text{bio}}$  ranging between  $1.1$  and  $1.9 \text{ L g}^{-1} \text{ d}^{-1}$ ) followed the kinetics described by the cometabolic model in our study, as suggested previously (see Section 3.1.2). With respect to biotransformation kinetics, only one study showed cometabolic biotransformation rate constants of up to  $2 \text{ L g}^{-1} \text{ d}^{-1}$  for carbamazepine in aerobic and anoxic activated sludge (Plósz et al., 2012). On the other hand biotransformations rate constants equal to  $0.9 \text{ L g}^{-1} \text{ d}^{-1}$  in aerobic MBBR have been reported (Escolà Casas et al., 2015a). In our study we thus observed 30 % removal of carbamazepine during batch experiments, which is in agreement with previous studies on MBBR (Escolà Casas et al., 2015a) and activated sludge (Dawas-Massalha et al., 2014; Luo et al., 2014; Zupanc et al., 2013). Thus, low removal of carbamazepine in the tested MBBRs in batch and continuous-flow experiments may be attributed to the limited transformation in the absence of primary substrates.

The biotransformation of the targeted sulfonamides was enhanced in the ethanol-dosed MBBR (up to 1.8-fold higher). As the ethanol-dosed MBBR showed the highest denitrification rates ( $r_{\text{NO}_{3,2-\text{N}}}$ ) during the batch experiment, the removal of the targeted sulfonamides may be associated with primary metabolism rather than biofilm composition (i.e., biodiversity). Interestingly, negative correlation between biotransformation kinetics of sulfonamides and biodiversity was also observed in nitrifying MBBRs, and their removal was enhanced at higher nitrification rates in thin biofilms (Torresi et al., 2016). Similarly, the removal of sulfamethoxazole has been previously shown to be dependent on the primary metabolism under anoxic condition in activated sludge, while negligible

effect of primary substrate was observed under nitrifying condition (Alvarino et al., 2016). This indicates that sulfonamide removal may be influenced by primary metabolism in both nitrifying and denitrifying conditions.

Finally, while  $k_{\text{bio}}$  of clarithromycin and erythromycin was found comparable to studies on aerobic MBBRs (Escolà Casas et al., 2015a), trimethoprim removal occurred with a higher  $k_{\text{bio}}$  under denitrification conditions than in aerobic MBBRs (Escolà Casas et al., 2015a; Falås et al., 2013).

### 3.5 Impact of carbon dosing during continuous-flow operation

A continuous-flow experiment tested different dosing conditions of organic carbon in terms of primary substrate (methanol or ethanol) and influent loading (variable  $\text{COD}_{\text{added}}/\text{NO}_3\text{-N}_{\text{influent}}$  ratio) without adaptation of the biofilm as described in Section 2.6 (details in Section S7, SI). The removal efficiency of micropollutants did not present any correlation with the tested  $\text{COD}_{\text{added}}/\text{NO}_3\text{-N}_{\text{influent}}$  ratios and did not significantly differ between the two types of carbon sources (Figure S8, SI). Notably, only trimethoprim removal increased with increasing carbon availability in the ethanol-dosed reactor.

Both MBBR systems exhibited denitrification rates directly proportional to the  $\text{COD}_{\text{added}}/\text{NO}_3\text{-N}_{\text{influent}}$  ratio (Figure S3, SI). However, at  $\text{COD}_{\text{added}}/\text{NO}_3\text{-N}_{\text{influent}}$  ratios higher than 4.8 and 3.8 for the methanol- and the ethanol-dosed MBBR, respectively, denitrification rates did not increase and similar effluent concentrations of COD were measured for both MBBRs (estimated to be equal to the inert soluble COD in the influent medium) (Figure S4, SI). This indicates that excess COD dosing during continuous-flow operation could have been used for internal storage rather than as primary energy source. This has been previously observed under substrate feast-famine cycles in

continuously operated activated sludge (Beun et al., 2000). Similarly, feast-famine conditions associated to change from high to low  $\text{COD}_{\text{added}}/\text{NO}_3\text{-N}_{\text{influent}}$  ratio during continuous-flow operation might have influenced the performance of the two post-denitrifying MBBRs in this study.

Furthermore, the continuous-flow operation experiment was carried out at HRT of 2 h, simulating HRTs typically operated in denitrification stages in full scale WWTPs, and which might have been too short to observe differences in the removal of micropollutants. In fact, the batch experiment showed that the removal of most of the targeted micropollutants (with the exception of the compounds removed through cometabolism) continued after 2 h from the start of the experiment (Figure 1), suggesting a possible removal enhancement at higher HRT. Accordingly, the increase of HRT has been found to enhance the removal of a number of micropollutants in activated sludge (Maurer et al., 2007; Petrie et al., 2014) and MBBR (Mazioti et al., 2015).

### **3.6. Comparison of the batch and the continuous-flow experiment**

Figure 4 compares the measured removal efficiencies under continuous –flow operation with the predicted removal efficiencies. The predicted values were calculated using the removal rates (k) estimated in the batch experiment according to first-order kinetics (Table 3). As presented in Figure 4, the removal rates (k) estimated from batch experiments allowed predicting of the elimination of most of the targeted compounds in continuous-flow operation. However, predicted removal efficiencies did not match the measurements for a number of micropollutants, i.e. sulfamethoxazole, carbamazepine, atenolol and trimethoprim. A possible explanation for this discrepancy might be that the removal rates (k) used to predict the removals were obtained by fitting the first order kinetics, while in reality for some compounds cometabolic or deconjugation approaches are more appropriate.



522

523 As the biotransformation kinetics of most of the compounds could be described with a first-order  
524 equation (Table 1, process 2 and Figure 1), it could be predicted that an HRT of 2 h (0.083 d) would  
525 only allow a partial removal of the easily biodegradable compounds (e.g., atenolol, trimethoprim  
526 and citalopram) in the continuous-flow experiment (Figure 4). For the compounds following this  
527 type of biotransformation kinetics, it could be predicted (Equation 1, Section 2.6) that the increase  
528 of the HRT up to 6 hours (0.25 d) would improve the removal efficiency by about 20%, achieving  
529 high removals in both reactors (>70%) for all the compounds listed as “easily biodegradable” in  
530 Table 3.

531

#### 532 **4. Conclusions**

533 In order to investigate the removal of micropollutants in denitrifying Moving Bed Biofilm Reactors  
534 (MBBRs), two laboratory-scale MBBRs were tested using nitrified effluent wastewater dosed with  
535 methanol and ethanol, respectively. The following conclusions have been drawn:

536

537 • According to the batch experiment, all targeted micropollutants showed biotransformation rate  
538 constants over  $0.2 \text{ L d}^{-1} \text{ g}_{\text{biomass}}^{-1}$  under denitrifying condition, except for diclofenac, phenazone,  
539 diatrizoic acid and iopamidol, which were found to be recalcitrant. Accordingly, it has been  
540 suggested that that HRTs of approximately 6 h could considerably enhance the removal of most  
541 of the targeted micropollutants.

542

543 • The biotransformation rate constants in the methanol-dosed MBBR were 1.5 to 2.5-fold higher  
544 than in the ethanol-dosed MBBR for 9 out of the 22 spiked pharmaceutical. Oppositely, the  
545 sulfonamides acetyl-sulfadiazine, sulfamethoxazole, sulfamethizole were transformed at higher

biotransformation rate constants in the ethanol-dosed MBBR. The rest of the compounds presented similar biotransformation in both reactors.

- The removal of venlafaxine, carbamazepine, sulfamethoxazole and sulfamethizole was most likely enhanced by the presence of organic growth substrates in the beginning of the batch experiment, suggesting cometabolic removal for these compounds.

- The continuous-flow experiment conducted at conditions typically operated in full-scale WWTPs (i.e., HRT = 2h) did not show significant correlation between the removal efficiency of micropollutants and the increase of carbon dosage or type.

## **5. Acknowledgements**

This research was supported by (i) the AUFF grant: advanced water purification using bio-inorganic nanocatalysts and soil filters; and (ii) MERMAID: an Initial Training Network funded by the People Programme (Marie-Curie Actions) of the European Union's Seventh Framework Programme FP7/2007-2013/ under REA grant agreement n. 607492. The authors are thankful for technical assistance provided by VA SYD at Sjölanda and Klagshamn (Malmö) wastewater treatment plants.

564 **References**

565

566 Alvarez-Cohen, L., Speitel, G.E., 2001. Kinetics of aerobic cometabolism of chlorinated solvents.  
567 Biodegradation 12 (2), 105–126.

568 Alvarino, T., Nastold, P., Suárez, S., Omil, F., Corvini, P.F.X., Bouju, H., 2016. Role of  
569 biotransformation, sorption and mineralization of 14C-labelled sulfamethoxazole under  
570 different redox conditions. Science of Total Environment 542, 706–715.

571 Alvarino, T., Suárez, S., Katsou, E., Vazquez-Padin, J., Lema, J.M., Omil, F., 2015. Removal of  
572 PPCPs from the sludge supernatant in a one stage nitrification/anammox process. Water  
573 Research. 68, 701–709. d

574 Anthony, C., 1982. The Biochemistry of Methylotrophs. Academic Press. London

575 Anthony, C., 2011. How half a century of research was required to understand bacterial growth on  
576 C1 and C2 compounds; the story of the serine cycle and the ethylmalonyl-CoA pathway.  
577 Science. Progress. 94, 109–37.

578 Bassin, J.P., Abbas, B., Vilela, C.L.S., Kleerebezem, R., Muyzer, G., Rosado, a. S., van  
579 Loosdrecht, M.C.M., Dezotti, M., 2015. Tracking the dynamics of heterotrophs and nitrifiers  
580 in moving-bed biofilm reactors operated at different COD/N ratios. Bioresource Technology  
581 192 (3), 131–141.

582 Baytshtok, V., Lu, H., Park, H., Kim, S., Yu, R., Chandran, K., 2009. Impact of varying electron  
583 donors on the molecular microbial ecology and biokinetics of methylotrophic denitrifying  
584 bacteria. Biotechnology and Bioengineering 102 (6), 1527–1536.

585 Beun, J.J., Paletta, F., Van Loosdrecht, M.C., Heijnen, J.J., 2000. Stoichiometry and kinetics of  
586 poly-beta-hydroxybutyrate metabolism in aerobic, slow growing, activated sludge cultures.  
587 *Biotechnology and Bioengineering* 67 (4), 379–89.

588 Biswas, K., Turner, S.J., 2012. Microbial community composition and dynamics of moving bed  
589 biofilm reactor systems treating municipal sewage. *Applied Environmental Microbiology* 78  
590 (3), 855–64.

591 Christensson, M., Lie, E., Welanders, T., 1944. A comparison between ethanol and methanol as  
592 carbon sources for denitrification. *Water Science and Technology* 30 (6), 83-90.

593 Clara, M., Strenn, B., Gans, O., Martinez, E., Kreuzinger, N., Kroiss, H., 2005. Removal of selected  
594 pharmaceuticals, fragrances and endocrine disrupting compounds in a membrane bioreactor  
595 and conventional wastewater treatment plants. *Water Research* 39 (19), 4797–807.

596 Criddle, C.S., 1993. The kinetics of cometabolism. *Biotechnology and Bioengineering* 41 (11),  
597 1048–56.

598 Cumming, G., Fidler, F., Vaux, D.L., 2007. Error bars in experimental biology. *Journal of Cell*  
599 *Biology* 177 (1), 7–11.

600 Dawas-Massalha, A., Gur-Reznik, S., Lerman, S., Sabbah, I., Dosoretz, C.G., 2014. Co-metabolic  
601 oxidation of pharmaceutical compounds by a nitrifying bacterial enrichment. *Bioresource and*  
602 *Technology*. 167, 336–42.

603 Delgadillo-Mirquez, L., Lardon, L., Steyer, J.P., Patureau, D., 2011. A new dynamic model for  
604 bioavailability and cometabolism of micropollutants during anaerobic digestion. *Water*  
605 *Research* 45 (15), 4511–4521.

606 Daughton, C.G., Ternes, T.A., 1999. Pharmaceuticals and personal care products in the  
607 environment: agents of subtle change? *Environmental Health Perspectives*. 907–38.

608 Escolà Casas, M.E., Chhetri, R.K., Ooi, G., Hansen, K.M.S., Litty, K., Christensson, M.,  
609 Kragelund, C., Andersen, H.R., Bester, K., 2015a. Biodegradation of pharmaceuticals in  
610 hospital wastewater by staged Moving Bed Biofilm Reactors (MBBR). *Water Research*. 83,  
611 293–302.

612 Escolà Casas, M., Chhetri, R.K., Ooi, G., Hansen, K.M.S., Litty, K., Christensson, M., Kragelund,  
613 C., Andersen, H.R., Bester, K., 2015b. Biodegradation of pharmaceuticals in hospital  
614 wastewater by a hybrid biofilm and activated sludge system (Hybas). *Science of Total*  
615 *Environment*. 530-531, 383–392.

616 Falås, P., Baillon-Dhumez, A., Andersen, H.R., Ledin, A la Cour Jansen, J., 2012. Suspended  
617 biofilm carrier and activated sludge removal of acidic pharmaceuticals. *Water Research*. 46  
618 (4), 1167–75.

619 Falås, P., Longrée, P., la Cour Jansen, J., Siegrist, H., Hollender, J., Joss, A, 2013. Micropollutant  
620 removal by attached and suspended growth in a hybrid biofilm-activated sludge process. *Water*  
621 *Research* 47 (13), 4498–506.

622 Fernandez-Fontaina, E., Carballa, M., Omil, F., Lema, J.M., 2014. Modelling cometabolic  
623 biotransformation of organic micropollutants in nitrifying reactors. *Water Research* 65C, 371–  
624 383.

625 Fischer, K., Majewsky, M., 2014. Cometabolic degradation of organic wastewater micropollutants  
626 by activated sludge and sludge-inherent microorganisms. *Applied Microbiology and*

627        Biotechnology 98 (15), 6583–97.

628   Göbel, A., McArdell, C.S., Joss, A., Siegrist, H., Giger, W., 2007. Fate of sulfonamides,  
629        macrolides, and trimethoprim in different wastewater treatment technologies. *Science of Total*  
630        *Environment* 372 (2-3), 361–371.

631   Hagman, M., Nielsen, J.L., Nielsen, P.H., La, J., Jansen, C., 2007. Mixed carbon sources for nitrate  
632        reduction in activated sludge-identification of bacteria and process activity studies. *Water*  
633        *Environmen Research* 42, 1539–1546

634   Hallin, S., Throbäck, I.N., Dicksved, J., Pell, M., 2006. Metabolic profiles and genetic diversity of  
635        denitrifying communities in activated sludge after addition of methanol or ethanol. *Applied*  
636        *Microbiology and Biotechnology* 72 (8), 5445–52.

637   Hapeshi, E., Lambrianides, A., Koutsoftas, P., Kastanos, E., Michael, C., Fatta-Kassinou, D., 2013.  
638        Investigating the fate of iodinated X-ray contrast media iohexol and diatrizoate during  
639        microbial degradation in an MBBR system treating urban wastewater. *Environmental Science*  
640        *and Pollution Research* 20 (6), 3592–606.

641   Hiatt, W.C., Grady, C.P.L., 2008. An Updated Process Model for Carbon Oxidation, Nitrification,  
642        and Denitrification. *Water Environmen Research* 80 (11), 2145–2156.

643   Hill, M., 1973. Diversity and evenness: a unifying notation and its consequences. *Ecology* 54 (2),  
644        427–432.

645   Jenkins, O., Byrom, D., Jones, D., 1987. *Methylophilus* - a New Genus of Methanol-Utilizing  
646        Bacteria. *International Journal of Systematic Bacteriology*. 37 (4), 446–448.

647 Johnson, D.R., Helbling, D.E., Lee, T.K., Park, J., Fenner, K., Kohler, H.P.E., Ackermann, M.,  
648 2015. Association of biodiversity with the rates of micropollutant biotransformations among  
649 full-scale wastewater treatment plant communities. *Applied and Environmental Microbiology*  
650 81 (2), 666–675.

651 Joss, A., Siegrist, H., Ternes, T.A., 2008. Are we about to upgrade wastewater treatment for  
652 removing organic micropollutants? *Water Science and Technology* 57, 251–5.

653 Joss, A., Zabczynski, S., Göbel, A., Hoffmann, B., Löffler, D., McArdell, C.S., Ternes, T. a.,  
654 Thomsen, A., Siegrist, H., 2006. Biological degradation of pharmaceuticals in municipal  
655 wastewater treatment: Proposing a classification scheme. *Water Research* 40 (8), 1686–1696.

656 Kassotaki, E., Buttiglieri, G., Ferrando-Climent, L., Rodriguez-Roda, I., Pijuan, M., 2016.  
657 Enhanced sulfamethoxazole degradation through ammonia oxidizing bacteria co-metabolism  
658 and fate of transformation products. *Water Research*.

659 Liu, L., Binning, P.J., Smets, B.F., 2015. Evaluating alternate biokinetic models for trace pollutant  
660 cometabolism. *Environmental Science and Technology* 49 (4), 2230–2236.

661 Louzeiro, N., 2002. Methanol-induced biological nutrient removal kinetics in a full-scale  
662 sequencing batch reactor. *Water Research*. 36 (11), 2721–2732.

663 Lu, H., Chandran, K., Stensel, D., 2014. Microbial ecology of denitrification in biological  
664 wastewater treatment. *Water Research*. 64, 237–254.

665 Luo, Y., Guo, W., Ngo, H.H., Nghiem, L.D., Hai, F.I., Kang, J., Xia, S., Zhang, Z., Price, W.E.,  
666 2014. Removal and fate of micropollutants in a sponge-based moving bed bioreactor.  
667 *Bioresource Technology* 159, 311–9.

668 Maurer, M., Escher, B.I., Richle, P., Schaffner, C., Alder, a C., 2007. Elimination of beta-blockers  
669 in sewage treatment plants. *Water Research*. 41 (7), 1614–22.

670 Mazioti, A. a., Stasinakis, A.S., Pantazi, Y., Andersen, H.R., 2015. Biodegradation of  
671 benzotriazoles and hydroxy-benzothiazole in wastewater by activated sludge and moving bed  
672 biofilm reactor systems. *Bioresource Technology* 192, 627–635.

673 Mokhayeri, Y., Riffat, R., Murthy, S., Bailey, W., Takacs, I., Bott, C., 2009. Balancing yield,  
674 kinetics and cost for three external carbon sources used for suspended growth post-  
675 denitrification. *Water Science and Technology* 60, 2485–91.

676 Müller, E., Schüssler, W., Horn, H., Lemmer, H., 2013. Aerobic biodegradation of the sulfonamide  
677 antibiotic sulfamethoxazole by activated sludge applied as co-substrate and sole carbon and  
678 nitrogen source. *Chemosphere* 92, 969–78.

679 Onesios, K.M., Yu, J.T., Bouwer, E.J., 2009. Biodegradation and removal of pharmaceuticals and  
680 personal care products in treatment systems: a review. *Biodegradation* 20 (4), 441–466.

681 Pan, Y., Ni, B.-J., Lu, H., Chandran, K., Richardson, D., Yuan, Z., 2015. Evaluating two concepts  
682 for the modelling of intermediates accumulation during biological denitrification in wastewater  
683 treatment. *Water Research*. 71, 21–31.

684 Petrie, B., McAdam, E.J., Lester, J.N., Cartmell, E., 2014. Assessing potential modifications to the  
685 activated sludge process to improve simultaneous removal of a diverse range of  
686 micropollutants. *Water Research*, 180-92.

687 Plósz, B.G., Benedetti, L., Daigger, G.T., Langford, K.H., Larsen, H.F., Monteith, H., Ort, C., Seth,  
688 R., Steyer, J.-P., Vanrolleghem, P. a, 2013. Modelling micro-pollutant fate in wastewater



689 collection and treatment systems: status and challenges. *Water Science and Technology* 67, 1–  
690 15.

691 Plósz, B.G., Langford, K.H., Thomas, K. V, 2012. An activated sludge modeling framework for  
692 xenobiotic trace chemicals (ASM-X): assessment of diclofenac and carbamazepine.  
693 *Biotechnology and Bioengineering* 109 (11), 2757–69.

694 Plósz, B.G., Leknes, H., Thomas, K. V, 2010. Impacts of competitive inhibition, parent compound  
695 formation and partitioning behavior on the removal of antibiotics in municipal wastewater  
696 treatment. *Environmental Science and Technology* 44 (2), 734–42.

697 Polesel, F., Andersen, H.R., Trapp, S., Plosz, B.G., 2016. Removal of antibiotics in biological  
698 wastewater treatment systems – A critical assessment using the Activated Sludge Modelling  
699 framework for Xenobiotics (ASM-X). *Environmental Science and Technology* 50 (19),  
700 10316–10334

701 Popat, S.C., Deshusses, M.A., 2011. Kinetics and inhibition of reductive dechlorination of  
702 trichloroethene, cis-1,2-dichloroethene and vinyl chloride in a continuously fed anaerobic  
703 biofilm reactor. *Environmental Science and Technology* 45 (84), 1569–1578.

704 Reichert, P., 1994. Aquasim - a tool for simulation and data-analysis of aquatic systems. *Water*  
705 *Science and Technology* 30 (2), 21 – 30.

706 Rittmann, B.E., 1992. Microbiological detoxification of hazardous organic contaminants: the  
707 crucial role of substrate interactions. *Water Science and Technology* 25, 403–410.

708 Roeleveld, P.J., Van Loosdrecht, M.C.M., 2002. Experience with guidelines for wastewater  
709 characterisation in The Netherlands. *Water Science and Technology* 45 (6), 77–87.

710 Santos, S.G., Zaiat, M., Varesche, M.B., Foresti, E., 2001. Comparative research on the use of  
 711 methanol , ethanol and methane as electron donors for denitrification. *Environmental*  
 712 *Engineering Science* 21 (39), 313-320.

713 Sözen, S., Çokgör, E.U., Orhon, D., Henze, M., 1998. Respirometric analysis of activated sludge  
 714 behaviour—II. Heterotrophic growth under aerobic and anoxic conditions. *Water Research*. 32,  
 715 476–488.

716 Stadler, L.B., Love, N.G., 2016. Impact of microbial physiology and microbial community structure  
 717 on pharmaceutical fate driven by dissolved oxygen concentration in nitrifying bioreactors.  
 718 *Water Research*. 104, 189–199.

719 Su, L., Aga, D., Chandran, K., Khunjar, W.O., 2015. Factors impacting biotransformation kinetics  
 720 of trace organic compounds in lab-scale activated sludge systems performing nitrification and  
 721 denitrification. *Journal Hazardous Material* 282, 116–24.

722 Suárez, S., Lema, J.M., Omil, F., 2010. Removal of Pharmaceutical and Personal Care Products (   
 723 PPCPs ) under nitrifying and denitrifying conditions. *Water Research* 44 (10), 3214–3224.

724 Suárez, S., Ramil, M., Omil, F., Lema, J.M., 2005. Removal of pharmaceutically active compounds  
 725 in nitrifying-denitrifying plants. *Water Science and Technology* 52 (8), 9–14.

726 Suárez, S., Reif, R., Lema, J.M., Omil, F., 2012. Mass balance of pharmaceutical and personal care  
 727 products in a pilot-scale single-sludge system: influence of T, SRT and recirculation ratio.  
 728 *Chemosphere* 89 (2), 164–71.

729 Torresi, E., Fowler, J.S., Polesel, F., Bester, K., Andersen, H.R., Smets, B.F., Plosz, B.G.,  
 730 Christensson, M., 2016. Biofilm thickness influences biodiversity in nitrifying MBBRs –

731 Implications on micropollutant removal. *Environmental Science and Technology*. 50 (17),  
732 9279–9288

733 Tran, N.H., Urase, T., Kusakabe, O., 2009. The characteristics of enriched nitrifier culture in the  
734 degradation of selected pharmaceutically active compounds. *Journal of Hazardous Material*  
735 171 (1-3), 1051–7.

736 Tran, N.H., Urase, T., Ngo, H.H., Hu, J., Ong, S.L., 2013. Insight into metabolic and cometabolic  
737 activities of autotrophic and heterotrophic microorganisms in the biodegradation of emerging  
738 trace organic contaminants. *Bioresource Technology*. 146, 721–31.

739 Vree, T.B., de Ven, E.S. van, Verwey-van Wissen, C.P.W.G.M., Baars, A.M., Swolfs, A., van  
740 Galen, P.M., Amatdjais-Groenen, H., 1995. Isolation, identification and determination of  
741 sulfadiazine and its hydroxy metabolites and conjugates from man and Rhesus monkey by  
742 high-performance liquid chromatography. *Journal of Chromatography B: Biomedical Sciences*  
743 and Applications 670 (1), 111–123.

744 Wittebolle, L., Marzorati, M., Clement, L., Balloi, A., Daffonchio, D., Heylen, K., De Vos, P.,  
745 Verstraete, W., Boon, N., 2009. Initial community evenness favours functionality under  
746 selective stress. *Nature* 458 (72238), 623–6.

747 Xia, S., Jia, R., Feng, F., Xie, K., Li, H., Jing, D., Xu, X., 2012. Effect of solids retention time on  
748 antibiotics removal performance and microbial communities in an A/O-MBR process.  
749 *Bioresource Technology*. 106, 36–43.

750 Zarfl, C., Klasmeier, J., Matthies, M., 2009. A conceptual model describing the fate of sulfadiazine  
751 and its metabolites observed in manure-amended soils. *Chemosphere* 77 (6), 720–726.

752 Zupanc, M., Kosjek, T., Petkovšek, M., Dular, M., Kompare, B., Širok, B., Blažeka, Ž., Heath, E.,  
753 2013. Removal of pharmaceuticals from wastewater by biological processes, hydrodynamic  
754 cavitation and UV treatment. *Ultrason. Sonochem.* 20, 1104–12.

755

756

757

758 **Web references**

759 EAWAG-BBD Pathway Prediction System. <http://eawag-bbd.ethz.ch/predict/index.html> (Accessed  
760 February 24, 2016). (2016)

761

762 **Tables**

763 **Table 1. Stoichiometric (Gujer) matrix of the ASM-X (which includes processes such as parent**  
764 **compound retransformation, biotransformation and the cometabolic model) and two-step denitrifying**  
765 **model used in this study.**  
766 **Stoichiometric coefficients:  $A = (1 - Y_H)/(1.143 * Y_H)$ ;  $B = (1 - Y_H)/(1.713 * Y_H)$ ;  $F$  = ratio between molecular**  
767 **mass of parent compound and metabolite undergoing deconjugation. Parameters and state variables**  
768 **for determination of micropollutant kinetics are described in the main text. Parameters and state**  
769 **variables for the denitrifying model are defined in Table S1 in Supplementary Information. For**  
770 **estimation of denitrification kinetics, biomass concentration  $X_H$  is expressed in  $\text{gCOD L}^{-1}$ ; \*Due to**  
771 **short duration of the batch experiment and low S/X ratio, negligible biomass growth was assumed.**  
772

(i) Component → i	C <sub>LI</sub>	C <sub>CJ</sub>	S <sub>NO3</sub>	S <sub>NO2</sub>	S <sub>N2</sub>	S <sub>s</sub>	X <sub>biomass</sub>	Process rate
(j)Processes ↓								
Micropollutants kinetics								
<sup>(1)</sup> <b>Parent compound retransformation</b>	F	-1						$\frac{k_{Dec} C_{CJ} X_{biomass}}{1 + K_D X_{biomass}}$
<sup>(2)</sup> <b>Biotransformation</b>	-1							$\frac{k_{bio} C_{LI} X_{biomass}}{1 + K_D X_{biomass}}$
<sup>(3)</sup> <b>Cometabolism</b>	-1							$\frac{q_{bio} (S_s/(S_s + K_S)) + k_{bio} C_{LI} X_{biomass}}{1 + K_D X_{biomass}}$
Denitrification kinetics								
<b>R1</b>		-A	+A		-1/Y <sub>H</sub>	*		$\mu_H \eta_{g1} X_H \frac{S_s}{K_{S1} * S_S} \frac{S_{NO3}}{K_{NO3}^{HB} * S_{NO3}}$
<b>R2</b>			-B	+B	-1/Y <sub>H</sub>	*		$\mu_H \eta_{g2} X_H \frac{S_s}{K_{S2} * S_S} \frac{S_{NO2}}{K_{NO2}^{HB} * S_{NO2}}$
R1: Anoxic growth of heterotrophs, reducing nitrate to nitrite (NO <sub>3</sub> <sup>-</sup> -> NO <sub>2</sub> <sup>-</sup> )								
R2: Anoxic growth of heterotrophs, reducing nitrite to nitrogen (NO <sub>2</sub> <sup>-</sup> -> N <sub>2</sub> )								

773

774

775 **Table 2. Values of denitrification rates normalized by carriers surface area ( $r_{\text{NO}_{3,2}\text{-N}}$ ) and biomass**  
776 **concentration ( $k_{\text{NO}_{3,2}\text{-N}}$ ) measured during batch experiments. SA: total surface area of carriers in the**  
777 **MBBRs.**  
778

MBBR	SA ( $\text{m}^2$ )	Biomass ( $\text{g L}^{-1}$ )	$r_{\text{NO}_{3,2}\text{-N}}$ ( $\text{gNO}_{3,2}\text{-N m}^{-2} \text{ d}^{-1}$ )	$k_{\text{NO}_{3,2}\text{-N}}$ ( $\text{gNO}_{3,2}\text{-N g}_{\text{biomass}}^{-1} \text{ d}^{-1}$ )
Methanol-dosed	0.2	3.28 $\pm$ 0.93	1.77 $\pm$ 0.92	0.11 $\pm$ 0.06
Ethanol-dosed	0.2	4.20 $\pm$ 0.25	2.32 $\pm$ 0.62	0.11 $\pm$ 0.03

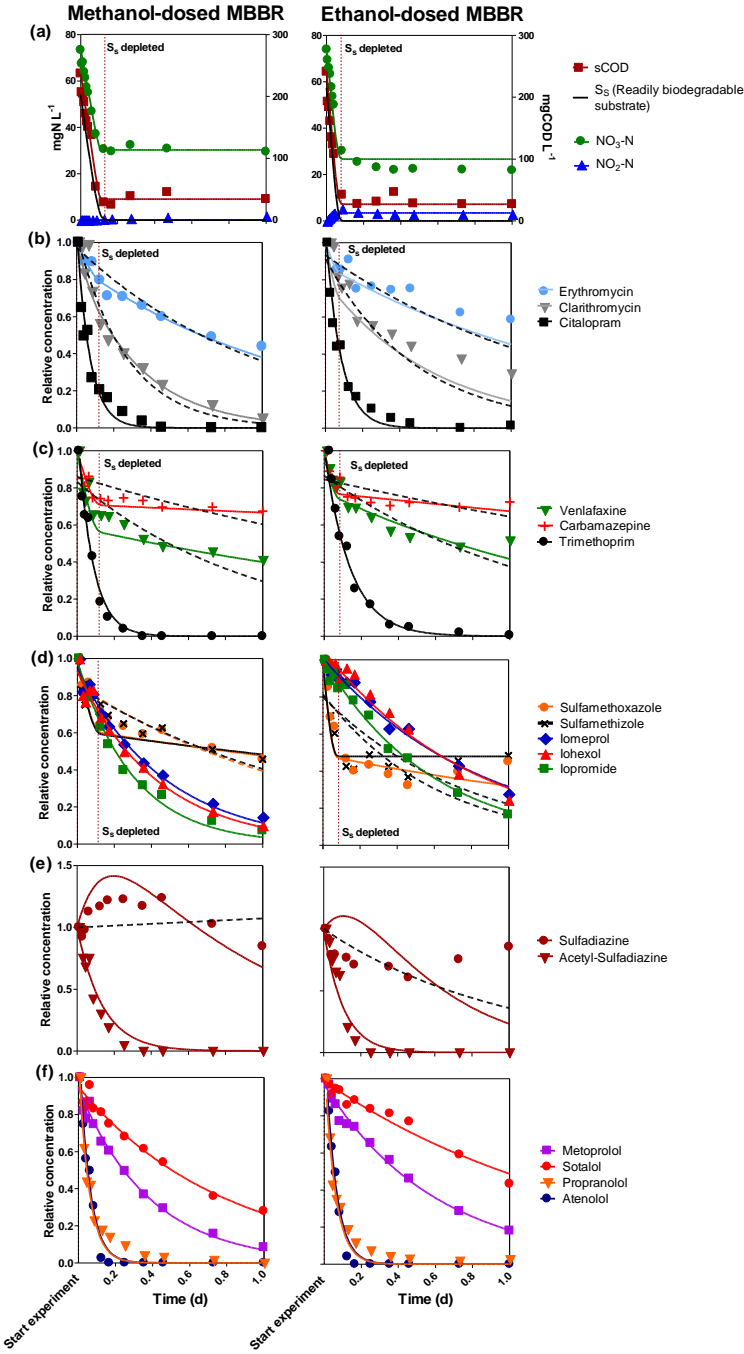
779

780

781 **Table 3. Values of  $k$ ,  $k_{bio}$ ,  $q_{bio}$  and  $k_{Dec}$  estimated for the two MBBRs from the data obtained in the**  
782 **batch experiments. “ $k$ ” defines the removal rate constant obtained following single first-order**  
783 **kinetics and not accounting for biomass concentration and sorption processes. “ $k_{bio}$ ” and “ $q_{bio}$ ” refer**  
784 **to removal rate constants normalized for biomass and sorption processes. Unindexed values**  
785 **correspond to “ $k_{bio}$ ” (Biotransformation process, Table 1, Process 2). Index (1) indicates the case of**  
786 **retransformation rate constant “ $k_{Dec}$ ” of acetyl-sulfadiazine to sulfadiazine (Transformation process,**  
787 **Table 1, Process 1). Index (2) refers to the cometabolic rate constant “ $q_{bio}$ ” (Cometabolism, Table 1,**  
788 **Process 3). The following abbreviations are used: n.d. = not degradable, SD =standard deviation.**  
789

Compound	Methanol-dosed MBBR		Ethanol-dosed MBBR	
	$k \pm SD$ ( $d^{-1}$ )	$k_{bio}, q_{bio} \pm SD$ ( $L d^{-1} g_{biomass}^{-1}$ )	$k \pm SD$ ( $d^{-1}$ )	$k_{bio}, q_{bio} \pm SD$ ( $L d^{-1} g_{biomass}^{-1}$ )
<b><i>Easily degradable; <math>k_{bio}, q_{bio} &gt; 2</math></i></b>				
Propranolol	$17.8 \pm 0.2$	$12.9 \pm 1.3$	$17.7 \pm 0.2$	$11.7 \pm 0.7$
Atenolol	$17.8 \pm 0.2$	$6.4 \pm 0.6$	$17.6 \pm 0.2$	$5.1 \pm 0.3$
Citalopram	$14.2 \pm 0.9$	$4.3 \pm 0.5$	$12.3 \pm 0.1$	$2.3 \pm 0.1$
Trimethoprim	$13.6 \pm 0.1$	$4.1 \pm 0.4$	$9.0 \pm 0.1$	$2.1 \pm 0.1$
Acetyl-sulfadiazine	$12.1 \pm 0.3$	$3.7 \pm 0.4^{(1)}$	$17.6 \pm 0.2$	$4.2 \pm 0.3^{(1)}$
<b><i>Moderately degradable; <math>0.2 \leq k_{bio}, q_{bio} \leq 2</math></i></b>				
Ibuprofen	$4.6 \pm 0.1$	$1.4 \pm 0.4$	$2.3 \pm 0.1$	$0.5 \pm 0.03$
Clarithromycin	$2.9 \pm 0.7$	$1.0 \pm 0.2^{(2)}$ $0.6 \pm 0.1$	$4.4 \pm 0.9$	$0.9 \pm 0.2^{(2)}$ $0.4 \pm 0.1$
Iopromide	$3.0 \pm 0.1$	$0.9 \pm 0.1$	$1.7 \pm 0.1$	$0.4 \pm 0.1$
Metoprolol	$2.6 \pm 0.1$	$0.8 \pm 0.2$	$1.7 \pm 0.1$	$0.4 \pm 0.03$
Iohexol	$2.3 \pm 0.1$	$0.7 \pm 0.2$	$1.2 \pm 0.1$	$0.3 \pm 0.1$
Iomeprol	$2.1 \pm 0.1$	$0.6 \pm 0.1$	$1.2 \pm 0.1$	$0.3 \pm 0.1$
Sotalol	$1.3 \pm 0.1$	$0.5 \pm 0.1$	$0.7 \pm 0.1$	$0.2 \pm 0.02$
Erythromycin	$1.5 \pm 0.1$	$0.5 \pm 0.1^{(2)}$ $0.2 \pm 0.1$	$2.5 \pm 0.1$	$0.6 \pm 0.1^{(2)}$ $0.2 \pm 0.1$
Venlafaxine	$6.0 \pm 0.1$	$1.9 \pm 0.2^{(2)}$ $0.1 \pm 0.1$	$4.8 \pm 0.1$	$1.1 \pm 0.1^{(2)}$ $0.1 \pm 0.1$
Carbamazepine	$3.9 \pm 0.1$	$1.2 \pm 0.3^{(2)}$ $0.1 \pm 0.1$	$4.6 \pm 0.1$	$1.1 \pm 0.1^{(2)}$ $0.1 \pm 0.1$
Sulfamethoxazole	$5.6 \pm 0.8$	$1.7 \pm 0.2^{(2)}$ $0.1 \pm 0.1$	$13.5 \pm 0.7$	$3.2 \pm 0.2^{(2)}$ $0.1 \pm 0.1$
Sulfamethizole	$5.8 \pm 0.9$	$1.8 \pm 0.2^{(2)}$ $0.1 \pm 0.1$	$13.8 \pm 0.8$	$3.3 \pm 0.2^{(2)}$ 0
Sulfadiazine	$1.9 \pm 0.2$	$0.6 \pm 0.1$	$4.2 \pm 0.6$	$1.0 \pm 0.2$
<b><i>Hardly or non-degradable; <math>k_{bio}, q_{bio} &lt; 0.2</math></i></b>				
Diatrizoic acid	$0.3 \pm 0.1$	$0.1 \pm 0.02$	$0.1 \pm 0.1$	$0.1 \pm 0.1$
Iopamidol	$0.2 \pm 0.1$	$0.1 \pm 0.02$	$0.1 \pm 0.1$	$0.1 \pm 0.1$
Diclofenac	n.d.	n.d.	n.d.	n.d.
Phenazone	n.d.	n.d.	n.d.	n.d.

790

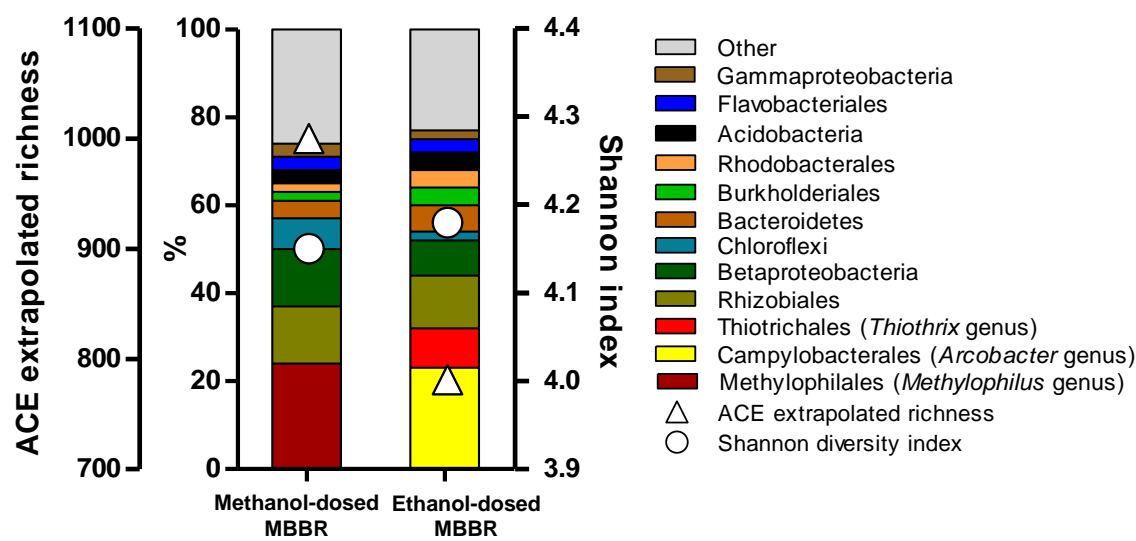


792

793 **Figure 1. Batch experiment results for selected compounds. On the X-axes “Time (d)” designates the sampling**  
794 **starting time-points. On the Y-axes “Relative concentration” refers to concentrations normalized to the measured**  
795 **starting concentrations. Symbols refer to measurements while lines refer to modelling. [a] Macro-pollutants.**  
796 **Readily biodegradable substrate (S<sub>s</sub>) is only modelled. [b-d] Solid lines: modelled concentrations assuming**  
797 **cometabolism (process 3, Table 1). Dashed lines: concentrations according to the biotransformation model**  
798 **(process 2, Table 1). [e] Solid lines: biotransformation-retransformation model (process 1, Table 1) assuming**  
799 **deconjugation of acetyl-sulfadiazine to sulfadiazine. Dashed lines: biotransformation model (process 2, Table**  
800 **1). [f] Solid lines: concentrations according to the biotransformation model (process 2, Table 1).**  
801



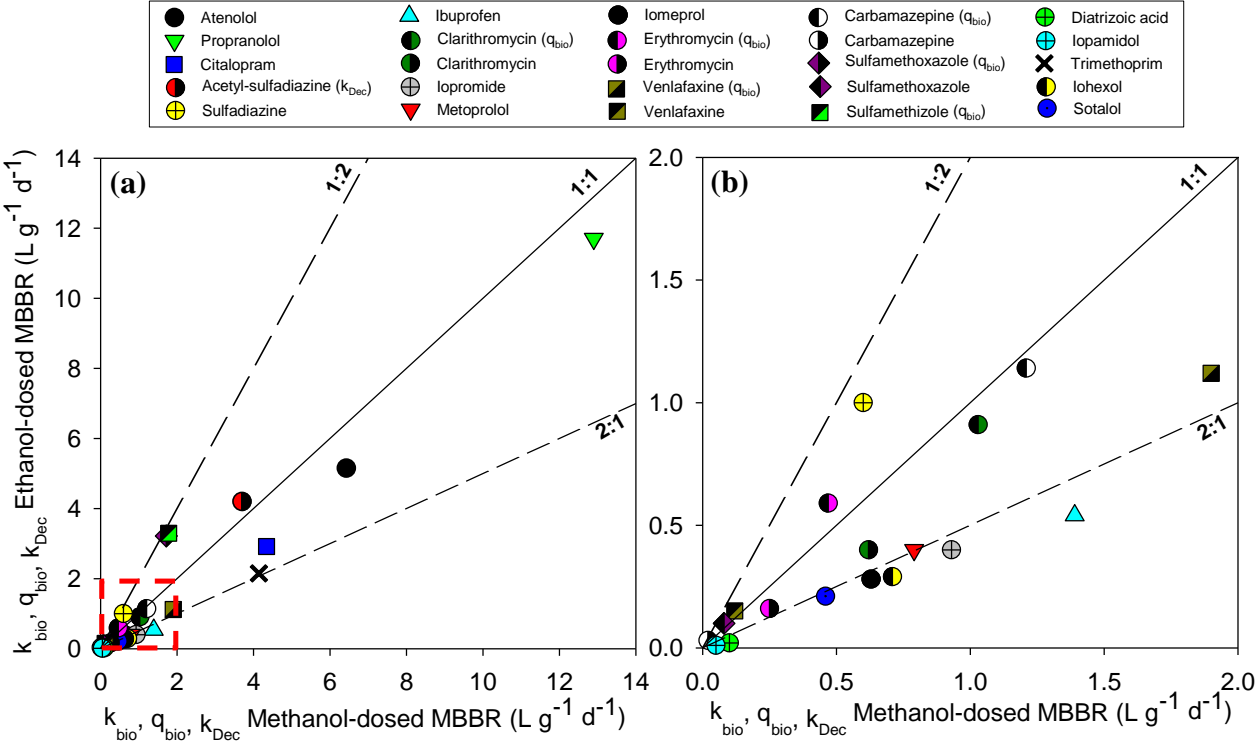
802



803

804 **Figure 2. Order-level taxonomic classification of 16S rRNA amplicons of the two MBBRs. The three**  
805 **most abundant orders are reported also at genus level (*Methylophilus*, *Arcobacter* and *Thiothrix*).**  
806 **Taxa abundance is expressed in percentage (second left axis). Alpha-diversity is measured as ACE**  
807 **extrapolated richness (first left axis) and Shannon diversity index (right axis).**

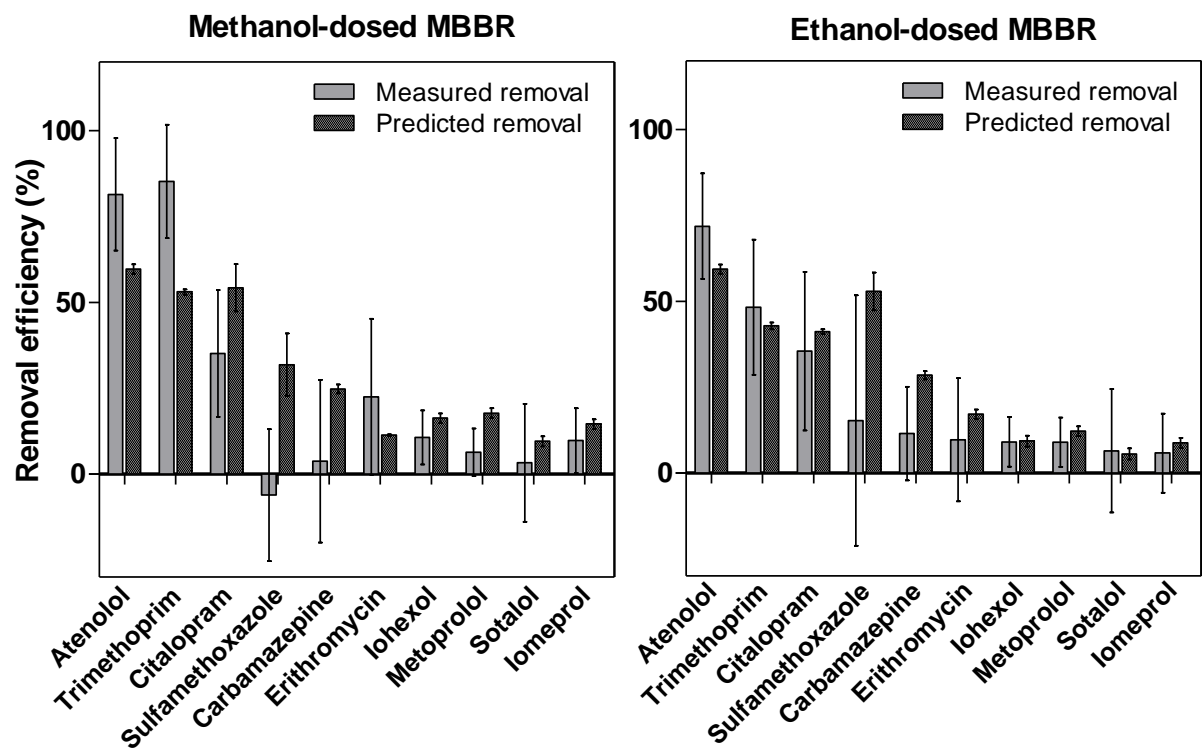
808



810

811 **Figure 3. Comparative assessment between methanol-dosed reactor (x-axes) and the ethanol-dosed**  
812 **reactor (y-axes) of the removal kinetics  $k_{bio}$ ,  $q_{bio}$  and  $k_{Dec}$  estimated for all targeted compounds (a) and**  
813 **for compounds with biokinetics ranging between 0 and 2 L g<sub>biomass</sub><sup>-1</sup> d<sup>-1</sup> (b). Dashed lines (2:1 and 1:2)**  
814 **delimit area where biokinetics are 2-fold higher or lower than other estimated values. In the legend,**  
815 **when not specified, symbols refer to estimated  $k_{bio}$ .**

816



818  
819 **Figure 4. Measured mean removal efficiency of micropollutants of all the tested  $COD_{added}/NO^3-N$**   
820 **influent ratios (presented in Table S3, SI) during the whole continuous-flow experiment, taking into**  
821 **account that no correlation was found between micropollutant removal and  $COD_{added}/NO^3-N$  influent**  
822 **ratios. The measured removals were calculated as difference between influent and effluent**  
823 **concentration, expressed as a percentage. Predicted removal was based on removal rate constants  $k$**   
824 **( $d^{-1}$ ) derived from batch experiments, calculated according to Equation 1 in Section 2.6.**  
825

826

827